

Orientation-dependent dissociative charge transfer

W. Wu and M. H. Prior

Chemical Sciences Division, Lawrence Berkeley National Laboratory, Berkeley, California 94720

H. Bräuning*

Department of Physics, Kansas State University, Manhattan, Kansas 66502

(Received 11 July 1997)

Recoil-ion momentum spectroscopy and molecular fragment imaging techniques are combined to study dissociative electron capture from He by HeH^+ at 0.20-a.u. collision velocity. Groups of final HeH states which dissociate to ground or excited H and He atoms are separated. For each group, the experiment provides two-dimensional H fragment distributions with respect to the collision plane and for fixed transverse momentum transfer. These patterns show that the capture probability is highest for HeH^+ ions with their axis oriented normal to the scattering plane for two of the three groups populated. [S1050-2947(98)50201-6]

PACS number(s): 34.70.+e, 82.30.Fi

HeH is an elementary diatomic molecule with a repulsive ground state, but many bound excited states [1–3]. The ground potential has been studied via H-He scattering [4], and bound excited states were established by emission spectroscopy in 1985 [5,6]. Since then, the electronic structure and the decay mechanism of the bound excited states, belonging to a Rydberg series associated with $\text{He}(1s^2\ ^1S) + \text{H}(nl)$ asymptotes (Fig. 1), have been studied by optical spectroscopy [7,8] and the kinetic energy of dissociating neutral fragments following charge transfer from alkali-metal atoms [9]. Recently, higher excited HeH states belonging to $\text{He}(1s2l) + \text{H}(1s)$ asymptotes have been studied via the dissociative recombination of HeH^+ with electrons [10,11].

This work reports a kinematically near-complete study of dissociative electron capture of HeH^+ from He, in which ground and excited states of HeH are formed. Combining cold-target recoil-ion momentum spectroscopy [12] with molecular fragment imaging, this experiment has obtained fragment distributions differentiated in kinetic energy of dissociation and molecular orientation for selected groups of HeH states and for fixed collision plane and momentum transfer. The term “near-complete” is used because the experiment determines a two-dimensional projection, onto a plane normal to the beam, of the three-dimensional fragment distribution. Fragments resulting from collision-induced dissociation of molecular ions [13] and electron capture from molecular targets [14] have been measured previously. This work differs in that the groups of dissociating molecular states are separated, and the vector momentum transfer of each collision is determined; the analysis then yields the molecular orientation dependence of the capture probability with respect to the scattering plane. Orientation dependence of excitation to dissociating states of the Na_2^+ has been reported recently by Brenot *et al.* [15], using a technique with some similarities to, but substantial differences from, the approach reported here.

A beam of 5-keV HeH^+ containing an undefined mixture of vibrational states was collimated to $1 \times 1 \text{ mm}^2$, and crossed by a cooled, supersonic He gas jet. Following the collision, charged projectile products were deflected electrostatically and HeH^+ ions were collected by a small Faraday cup. The neutral products from the collision were detected by a position-sensitive detector. The flight time for 5-keV HeH to reach the projectile detector from the interaction region was 480 ns, far larger than the dissociation lifetime [2]

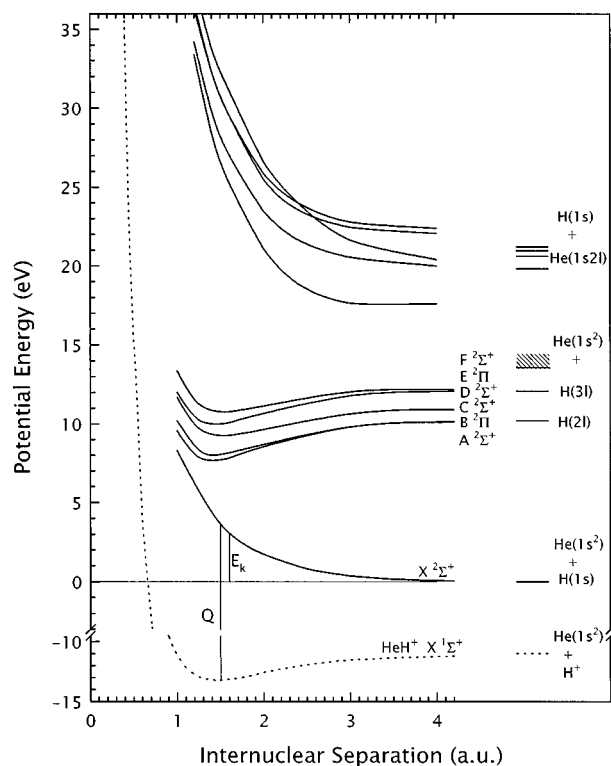


FIG. 1. Potential-energy curves of HeH ([2,3,18]) and HeH^+ ([23]) relevant to the present study. The change of target electronic energy from the initial $\text{HeH}^+ + \text{He}$ to the final $\text{HeH} + \text{He}^+$ system has been included, which shifts the energy curve of HeH^+ below HeH. The zero energy corresponds to $\text{He}(1s^2\ ^1S) + \text{H}(1s) + \text{He}^+$.

*On leave from the Institut für Kernphysik, Universität Frankfurt. Present address: Lawrence Berkeley National Laboratory, Berkeley, CA 94720.

of the HeH states populated in the collision. By using a rectangular mask that extended 2 mm beyond the neutral beam center, only one of the two neutral fragments from each dissociation event could strike the detector. The associated He^+ recoil ion was projected at right angles to the beam onto another position-sensitive detector by a weak extraction field (15 V/cm) followed by a field-free drift region. From the position and the time of flight of the recoil ion, measured by a coincidence with a projectile fragment, the recoil-ion momentum vector was determined [12]. The energy loss of the collision, Q , was calculated from the recoil-ion longitudinal momentum P_{\parallel} , as $Q = P_{\parallel}v + v^2/2$; v is the projectile velocity (all quantities in atomic units) [12].

For a HeH molecule formed at a distance L from the projectile detector, with its internuclear axis oriented at an angle θ relative to the beam direction and a kinetic-energy release E_k in its rest frame from the dissociation, the radial distance R on the detector of the H fragment from the center of mass of the He-H fragment pair is (to first order) $R(\theta) = R_k \sin \theta$, where $R_k = L[(m_{\text{He}}/m_{\text{H}})(E_k/E_b)]^{1/2}$ is the maximum distance occurring for $\theta=90^\circ$. Here E_b is the beam energy and m_{H} and m_{He} are the fragment masses for H and He. Interchanging m_{H} and m_{He} yields the R for the He fragment, one-fourth that for the H fragment. The center of mass of the HeH fragment pairs on the detector deviates from the beam center due to the scattering from the target. The significant scattering deviation was corrected in the analysis using the measured recoil-ion transverse momentum for each event. The beam center was found by using an attenuated HeH^+ beam on the unmasked projectile detector with the postcollision deflector switched off and half of the extraction field applied in the recoil-ion spectrometer.

Because the derivative of $R(\theta)$ with respect to θ is proportional to $\cos \theta$ and hence is zero for $\theta=90^\circ$, for a discrete kinetic-energy release, the R distribution is peaked at a radius very nearly equal to R_k . Therefore, the measured fragment position can be used to determine the kinetic-energy release [16,17]. However, the peak near R_k in the R distribution reflects only dissociations from molecules oriented near the $\theta=90^\circ$ plane, i.e., the plane normal to the beam. The measured R distribution is shown in Fig. 2(b) as a function of the energy loss Q , determined from the coincident He^+ recoil-ion momentum P_{\parallel} . Figure 2(a) shows the loci in the R_k - Q plane along which events should cluster for population of the HeH levels shown in Fig. 1. R_k is the radius of the fragment sphere computed from the dissociation energies derived from the theoretical energy-level curves (Fig. 1) and the flight time to the fragment detector. Figure 2(c) is a histogram from the projection of Fig. 2(b) onto the Q axis; the distribution is dominated by three groups at $Q=17$, 23, and 41 eV. They represent three groups of HeH states, the ground state, low-lying bound states, and higher excited states (cf. Fig. 1), populated in the capture process. Along the vertical R axis, the distribution contains two groups, one at smaller R (<4 mm), mainly the He fragments, and the other at larger R , dominated by the H fragments. [He fragments in this region would correspond to a kinetic-energy release larger than 11 eV, an unlikely process (Fig. 1).] The two groups are about a factor of 4 apart, as expected.

Starting from the low-energy loss side, the first group in Fig. 2(c) is from direct capture into the HeH ground state.

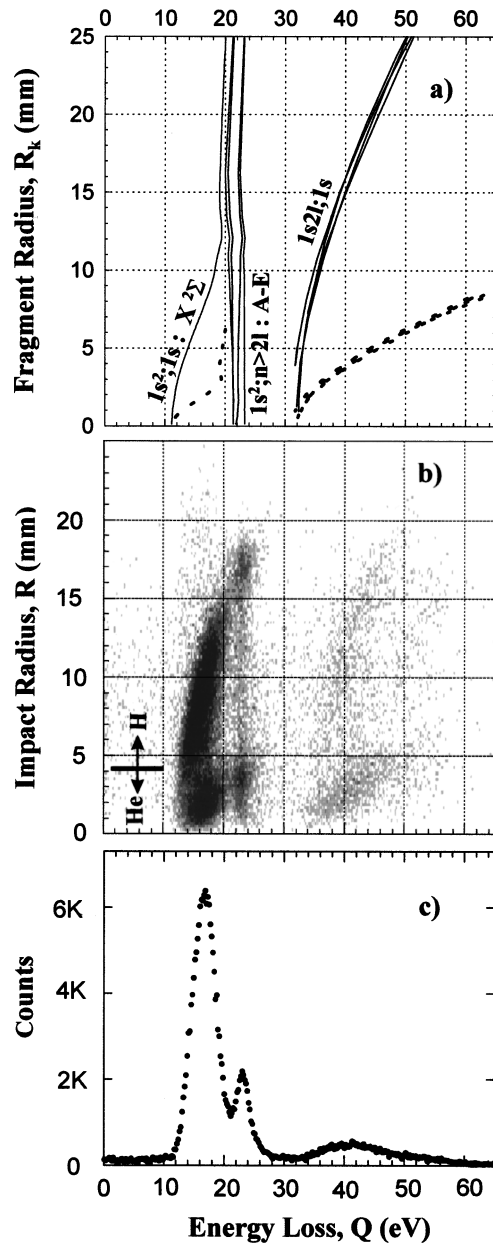


FIG. 2. (a) Loci of R_k vs Q expected for the potential curves shown in Fig. 1; solid (dotted) lines are for H (He) fragments. The labels on the solid curves include the asymptotic He, H configurations. The loci labeled $1s^2; n>2l$ are drawn assuming these levels predissociate via the molecular ground potential. (b) Density plot of the observed fragment radial distance (R) vs collision energy loss (Q); note the similarity to (a). Impacts with the $R>4$ mm are H fragments; those with $R<4$ mm are He fragments. (c) is a histogram formed by projecting (b) onto the Q axis.

The experimental resolution for the energy loss is measured to be 1 eV (full width at the half maximum). The broader energy-loss distribution at fixed R is caused by transitions from different initial vibrational states of HeH^+ . The presence of different initial vibrational states is also reflected in the observed R - Q correlation, because it allows the vertical transition to occur over a wide range of internuclear separations of the molecule. Transition from HeH^+ to HeH at smaller internuclear separation requires more energy (larger energy loss), but provides larger kinetic-energy release in the

subsequent dissociation (cf. Fig. 1).

The next group at $Q=23$ eV is from population of the bound excited HeH states associated with the $\text{He}(1s^2\ ^1S) + \text{H}(nl)$ asymptotes. Individual states are not distinguished with the present energy resolution. The R - Q correlation seen for the ground state is absent for these states, as their lifetimes, between 10^{-12} and 10^{-9} s, are much longer than the vibrational period ($\sim 10^{-15}$ s) [2]. Thus the transition and the dissociation take place at different internuclear separations without correlation. Compared to the dissociation of the ground state, the kinetic-energy release from these states is larger. This is direct evidence that these states decay via predissociation, by interaction with the $\text{He}(1s^2\ ^2S) + \text{H}(1s)$ ground state. Radiative dissociation, radiative decay to the ground state followed by dissociation of the ground state, yields the same kinetic-energy release as that for the ground state. Weaker intensity is seen at smaller R due to the radiative dissociation. The observation agrees with the theoretical prediction [2] and an earlier experiment [9].

The distribution at $Q=41$ eV is from the higher excited states of HeH belonging to a group that has $\text{He}(1s2l) + \text{H}(1s)$ asymptotes. These states are bound but with equilibrium separations >3.5 a.u. [3], far outside the 1.5-a.u. value for HeH^+ . Population of these states may require both the charge transfer and the excitation of the projectile HeH^+ [18]. Excitation of molecular ions in keV-energy collisions has been previously studied [15,19]; however, excitation of HeH^+ leaving a neutral He recoil is not measured in the present experiment, which requires a He^+ recoil ion. In the internuclear range where a vertical transition from HeH^+ can take place, these states dissociate, leading to neutral $\text{He}(1s2l)$ and $\text{H}(1s)$ fragments, with a kinetic-energy release of a few eV (Fig. 1). Alternatively, they can autoionize by reemitting an electron. However, this branch is weak for these states because they are so steeply repulsive in the Franck-Condon region of HeH^+ (cf. Fig. 1).

Figure 3 shows the fragment distributions projected onto the plane normal to the beam for the different HeH groups and for selected transverse momenta. Molecular orientation is meaningful only with respect to the beam direction and the direction of momentum transfer. The coordinate system for Fig. 3 is defined with the z axis in the direction of the beam and the x axis in the direction of the transverse momentum transfer (P_{\perp}). The scattering plane, determined by the beam axis and the recoil-ion momentum, is then the x - z plane. The distributions shown are the directly measured fragment distributions replotted relative to the scattering plane, which, though randomly oriented in the laboratory, is defined by the measurements for each event. Note from the previous discussion that the present measurement is not sensitive to molecules aligned on or near the beam direction ($\theta=0$); the distributions in the outermost region in R are H fragments dissociated from molecules oriented nearly perpendicular to the beam ($\theta=90^\circ$). As Fig. 3 shows, the fragment distributions are strongly anisotropic with respect to ϕ (the orientation angle with respect to the x axis) for HeH formed in the ground [Fig. 3(a)] and higher excited states [Fig. 3(c)]. On the other hand, for HeH formed in the low-lying bound states [Fig. 3(b)], fragments are distributed roughly isotropically with respect to the scattering plane. Since HeH formed in the repulsive ground state or higher excited states, which are also

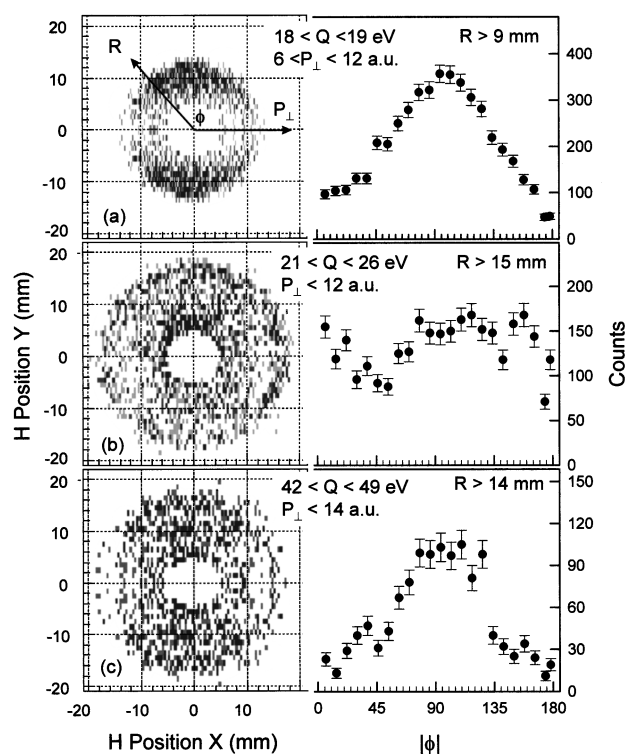


FIG. 3. Left, fragment distributions projected into the plane normal to the beam direction for HeH states formed in the ground (a), low-lying bound states (b), and higher excited states (c) in selected recoil-ion transverse momentum ranges. The scattering plane is defined by the beam axis (z) and the recoil-ion transverse momentum vector \mathbf{P}_{\perp} (x). Events in $R < 5$ -mm region are cut out. Right, the corresponding $|\phi|$ distribution for the outermost ring of the two-dimensional distribution.

repulsive in the Franck-Condon region of the initial HeH^+ , dissociates in a time small compared to the molecular rotation period, the fragment patterns directly reflect the HeH^+ orientation when the electron transfer occurs. Thus, Figs. 3(a) and 3(c) indicate that HeH^+ , whose internuclear axis is perpendicular to the scattering plane, is more likely to capture an electron from the target. For the low-lying bound excited states, however, an anisotropic capture process will not be observed in the fragment distribution. The lifetime for these states is of the order of 10^{-12} s for the $A^2\Sigma^+$ state and 10^{-9} s for other states [2], but the molecular rotation period is estimated to be of the order of 10^{-13} s. Thus any anisotropy for this capture channel is washed out by large random rotations before the dissociation occurs. Since the two nuclei differ in HeH^+ , there could be an asymmetry favoring momentum transfer towards one end of the molecule. This would shift the distribution in Figs. 3(a) and 3(c) away from $\phi=90^\circ$. Our results show that this is not a large effect. However, residual systematic uncertainties leave room for such an effect that is sizable enough to be revealed in future improved studies.

Angular anisotropy has been observed in dissociative recombination of molecular ions with free electrons [17,20,21] and electron capture from molecular targets [14]. There are two key differences between those measurements and the present one. First, the angular anisotropy observed in those experiments is with respect to the angle between the molecu-

lar axis and the beam. A propensity rule based on symmetry arguments [22] can partially explain the anisotropy for dissociative recombination, and the feature in electron capture by O^{8+} from H_2 can be qualitatively understood as the interference of capture amplitudes from the two atomic centers in H_2 [14]. Second, at a collision velocity of 0.2 a.u., the present experiment requires a quasimolecular approach, and cannot be treated either as dissociative recombination in a quasi-free-electron approach or in a perturbative approximation as used for electron capture at high velocity ($v \gg 1$ a.u.) [14].

In summary, a kinematically near-complete study of dissociative electron capture of HeH^+ from He has revealed the population and decay mechanisms of HeH molecules formed in different groups of states. The low-lying bound excited states are observed to be predissociative, while the higher excited states of HeH dissociate before autoionizing when formed at internuclear separations around 1 a.u. The two-

dimensional fragment distributions show that electron capture is strongest to HeH^+ ions with internuclear axes perpendicular to the scattering plane, for channels yielding ground and the higher excited HeH states. The results show that recoil-ion momentum spectroscopy combined with coincident fragment imaging can be a useful tool in studies of an interesting class of molecular ion-atom reactions.

The authors thank I. Ben-Itzhak, C. L. Cocke, S. Datz, and T. Osipov for helpful discussions, and Z. Xie of the LBNL Nuclear Science Division for valuable assistance. They also acknowledge assistance from Dr. R. Dörner and Dr. V. Mergel with the design and operation of the recoil-ion spectrometer. This work was supported by the Division of Chemical Sciences, Office of Basic Energy Sciences, Office of Energy Research, U.S. Department of Energy, Contract No. DE-AC03-765F00098. H.B. gratefully acknowledges support from the Alexander von Humboldt Foundation.

-
- [1] H.H. Michels and F.E. Harris, *J. Chem. Phys.* **39**, 1464 (1963).
 [2] G. Theodorakopoulos *et al.*, *J. Phys. B* **17**, 1453 (1984); I. D. Petsalakis, G. Theodorakopoulos, and R. J. Buenker, *Phys. Rev. A* **38**, 4004 (1988).
 [3] W.M. Miller and H. F. Schaeffer, *J. Chem. Phys.* **53**, 1421 (1970).
 [4] R. Gengenbach, Ch. Hahn, and J.P. Toennies, *Phys. Rev. A* **7**, 98 (1973); J.P. Toennies, W. Wels, and G. Wolf, *Chem. Phys. Lett.* **44**, 5 (1976).
 [5] T. Möller, M. Beland, and G. Zimmerer, *Phys. Rev. Lett.* **55**, 2145 (1985).
 [6] W. Ketterle, H. Figger, and H. Walther, *Phys. Rev. Lett.* **55**, 2941 (1985).
 [7] R.L. Brook, J.L. Hunt, and J.J. Miller, *Phys. Rev. Lett.* **58**, 199 (1987); D.W. Tokaryk, R.L. Brook, and J.L. Hunt, *Phys. Rev. A* **40**, 6113 (1989).
 [8] W. Ketterle, *Phys. Rev. Lett.* **62**, 1480 (1989).
 [9] W.J. van der Zande *et al.*, *Phys. Rev. Lett.* **57**, 1219 (1986).
 [10] T. Tanaba, I. Katayama, N. Inoue, K. Chida, Y. Arakaki, T. Watanabe, M. Yoshizawa, S. Ohtani, and K. Noda, *Phys. Rev. Lett.* **70**, 422 (1993); T. Tanaba, I. Katayama, N. Inoue, K. Chida, Y. Arakaki, T. Watanabe, M. Yoshizawa, M. Saito, Y. Haruyama, K. Hosono, T. Honma, K. Noda, S. Ohtani, and H. Takagi, *Phys. Rev. A* **49**, R1531 (1994).
 [11] G. Sundström *et al.*, *Phys. Rev. A* **50**, R2806 (1994); C. Strömholmit *et al.*, *ibid.* **54**, 3086 (1996).
 [12] J. Ullrich *et al.*, *Comments At. Mol. Phys.* **30**, 285 (1994); V. Mergel *et al.*, *Phys. Rev. Lett.* **74**, 2200 (1995).
 [13] E.P. Kanter *et al.*, *Phys. Rev. A* **20**, 834 (1979).
 [14] S. Cheng *et al.*, *Phys. Rev. A* **47**, 3923 (1993).
 [15] J.C. Brenot *et al.*, *Phys. Rev. Lett.* **77**, 1246 (1996).
 [16] D.P. de Bruijn and J. Los, *Rev. Sci. Instrum.* **53**, 1020 (1982).
 [17] D. Zajfman *et al.*, *Phys. Rev. Lett.* **75**, 814 (1995).
 [18] A.E. Orel, K.C. Kulander, and T.N. Rescigno, *Phys. Rev. Lett.* **74**, 4807 (1995).
 [19] D.H. Jaecks *et al.*, *Phys. Rev. Lett.* **50**, 825 (1983); D. Calabrese *et al.*, *Phys. Rev. A* **50**, 4899 (1994).
 [20] J. Semaniak *et al.*, *Phys. Rev. A* **54**, R4617 (1996).
 [21] Z. Amitay *et al.*, *Phys. Rev. A* **54**, 4032 (1996).
 [22] G.H. Dunn, *Phys. Rev. Lett.* **8**, 62 (1962).
 [23] T.A. Green *et al.*, *J. Chem. Phys.* **61**, 5186 (1974).